ACS OMEGA

Article

Cite This: ACS Omega 2018, 3, 18170−18180

http://pubs.acs.org/journal/acsodf

Experimental and Computational Evidence for "Double Pancake Bonds": The Role of Dispersion-Corrected DFT Methods in Strongly Dimerized 5-Aryl-1λ^2,3λ^2-dithia-2,4,6-triazines

René T. Boeré*

Department of Chemistry and Biochemistry and Canadian Centre for Research in Advanced Fluorine Technologies, University of Lethbridge, 4401 University Drive West, Lethbridge, Alberta, Canada T1K 3M4

Supporting Information

ABSTRACT: Crystal structures are reported for bicyclic 3-$CF_3C_6H_4CN_5S_3$ and monocyclic 3-$CF_3C_6H_4CN_3S_2$, the latter of which is strongly dimerized in a *cis*-cofacial geometry [3-$CF_3C_6H_4CN_3S_2$]$_2$. The title compounds have previously been characterized in solution by NMR, displaying spectra that are consistent with the structure of [3-$CF_3C_6H_4CN_3S_2$]$_2$ in the crystal with *anti*-oriented CF_3 substituents. The interannular binding was investigated using density functional theory (DFT) methods. However, the DFT-optimized geometry spreads the aryl rings too far apart (centroid−centroid distances of ≥4.353 Å versus experimental distance of 3.850 Å). Significant improvements are obtained with dispersion-corrected DFT functionals B3LYP-D3, B3LYP-D3BJ, M062X, and APFD using the 6-311+G(2d,p) basis set. However, all of these overbind the aryl rings with centroid−centroid distances of 3.612, 3.570, 3.526, and 3.511 Å, respectively. After selecting B3LYP-D3BJ/6-311+G(2d,p) as the best method, five alternative dimer geometries were tested, and all were found to be binding; however, *anti* cofacial-4 (matching the structure in the solid state) is the most stable. Computed energies of the remainder are as follows: +7.0 kJ mol^{-1} (*syn*-cofacial-5), +26.7 kJ mol^{-1} (*anti*-cofacial-64), +27.0 kJ mol^{-1} (*syn*-cofacial-150), +102.0 kJ mol^{-1} (S,S-antarafacial), and +103.7 kJ mol^{-1} (S,N-antarafacial), where the suffixes are torsional angles around the CN_3S_2 thiazyl ring centroids. The binding in the four most stable cofacial dimers may be described by "double pancake bonding".

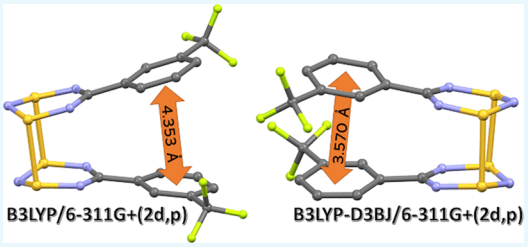

INTRODUCTION

Pancake bonding (PB), is an evocative name for two-electron/multicenter (2*e*/mc) bonding between π-stacked dimers of organic and light-atom radicals. This terminology was apparently introduced quite casually by Mulliken and Person back in 1969,[1] was revived in this century by Suzuki et al.,[2] and has since become popular.[3−23] Several reviews are available on the PB concept,[24,25] which should be distinguished from dispersion interactions in conventional "π-stacking" between diamagnetic aromatic rings, which is strictly due to London forces. By contrast, PB involves maximizing overlap of the (delocalized) π-somos (singly occupied molecular orbitals), which can be observed in the relative orientation of the atoms of the combining rings (and hence of any substituents). Although originally introduced to deal with hydrocarbons, PB is now also commonly used for heterocyclic thiazyls.[24,25] For example, three of the five experimentally validated geometries, whereby planar and thermally stable 1λ^2,2λ^2-dithia-3,5-diazolyl (DTDA) radicals associate into dimers, "lock in" to maximize the overlap of the π-somos of the monomeric species (**I**−**III** in Scheme 1).[24,26]

However, the heteroatom character of DTDAs and the inclusion of the third-period element S promote certain motifs such as *trans*-antarafacial **IV** and orthogonal **V**, which are not classified as PB in hydrocarbon radicals. These latter modes in DTDAs are rare and have only been confirmed crystallographically in rather complex mixed-configuration structures; the driving force for these latter associations could be primarily spin pairing of the radicals. Intriguingly, Beneberu et al. showed that the computed PB interaction energies in DTDAs follow the sequence **I** > **II** > **III** ≈ **IV** for HCN_2S_2 (**V** was not considered), illustrating the dominance of the orbital interactions by the greater overlap between the larger and more diffuse p orbitals of S compared to N and C.[6] That is, just two long S···S contacts appear to provide as much binding

Scheme 1. Five Dimerization Modes of 4-*R*-1,2,3,5-Dithiadiazolyl Dimers Showing the $\pi^*-\pi^*$ Interactions: *cis*-Cofacial I, Cofacial-90 II, *trans*-Cofacial III, *trans*-Antarafacial IV, and Orthogonal V

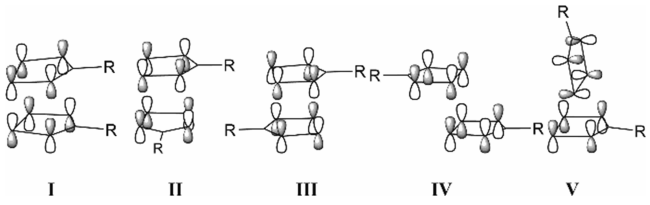

Received: November 18, 2018
Accepted: December 11, 2018
Published: December 24, 2018

energy as a full face-to-face ring interaction in **III**, where these are all of the S···N type.[6] Also significant for the DTDA study is the availability of crystal structures for prototypical HCN_2S_2—this is a real molecule that has been investigated both as a monomeric radical and a diamagnetic dimer.[27−29] Importantly, evidence for dimerization of DTDAs in solution has also been obtained from electron paramagnetic resonance (EPR) and UV−vis spectroscopies.[30,31]

PB is relatively weak (estimated at −75 kJ mol^{-1} for **I**), involving maximally 2*e* spread over many atoms, and is further weakened by the small stabilization that results when the rings bond without atom rehybridization (to preserve aromatic delocalization). The small HOMO−LUMO gap in PB dimers results in significant diradicaloid character (estimated at 0.32*e* for **I** by multiconfigurational self-consistent field (MCSCF) calculations), further reducing the net bonding *e* density. Moreover, the combining species are, in general, persistent free radicals that usually can exist independent of their dimers, so they are also good leaving groups. PB is a popular concept, because it captures all these characteristics in a simple heuristic approach that also has a pedagogical value. However, the essence of the idea was captured much earlier by "diffuse $\pi^*-\pi^*$ overlap" to explain many interactions in electron-rich, unsaturated thiazyl (i.e., −S˙=N−) compounds.[32] As introduced, this concept was a unifying framework for many interactions between such electron-rich unsaturated moieties, whether diamagnetic or paramagnetic (for example, it rationalizes the formation of transannular short contacts in thiazyl cage compounds such as the paradigmatic S_4N_4 structure).[31] Significantly, diffuse $\pi^*-\pi^*$ overlap was also used to develop the dimerization of the (formally antiaromatic) 8π 5-phenyl-1λ^2,3λ^2-dithia-2,4,6-triazine, wherein the very short transannular contacts were rationalized through four-electron multicenter (4*e*/mc) interactions (Figure 1).[33,34]

Kertesz and co-workers recently coined the term "double pancake bonding" (DPB) to describe such 4*e*/mc bonding between cofacial electron-rich ring systems as a conceptual extension of 2*e*/mc PB through in-depth computational work using a combination of complete active space (CASSCF) and multireference average quadratic coupled cluster (MR-AQCC),[35] as well as a large number of density functional theory (DFT) methods.[15,35] To date, these workers have only considered a *cis*-cofacial bonding motif (analogous to **I**) and restrict their investigations to the $[HCN_3S_2]_2$ dimer, which, for this heterocycle, is only a hypothetical model system. Unlike for the corresponding DTDA and for $H_2C_2N_4S_2$,[36] experimental routes to the parent heterocycle have not been worked out for DTTAs and would face significant obstacles from the high acidity of the hydrogen site. DPB has also been applied to boron and nitrogen-substituted phenalenyls (PLYs),[37] mimicking the extensive use of single PBs to all-carbon PLY dimers.[24] To date, just two 1λ^2,3λ^2-dithia-2,4,6-triazine (DTTA) dimers,[34,38] **1** and **2** (Chart 1), have been structurally characterized, and both exist as *cis*-cofacial dimers with short S···S contacts, which, at a mean of 2.571 Å, far exceed standard covalent bond distances (2.04 Å) but are also much less than $\sum r_{vdW}$ = 3.35 Å.[39]

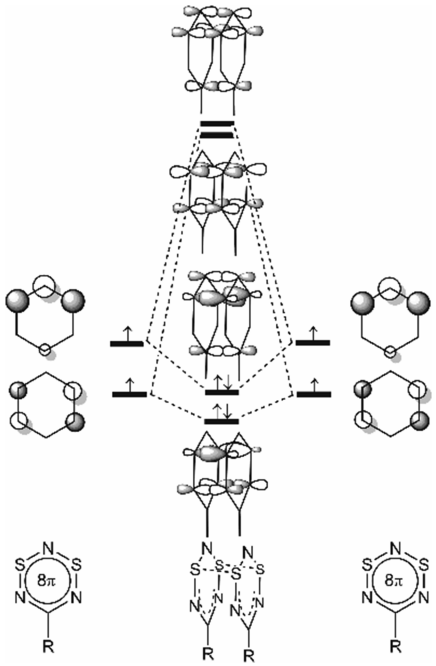

Figure 1. Diffuse $\pi^*-\pi^*$ bonding between 8π antiaromatic thiazyl heterocycles.

Chart 1. Structures of DTTA Dimers 1−3

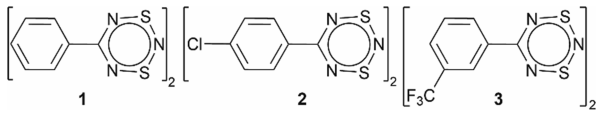

Recently, Haberhauer and Gleiter, also using only computational methods (DFT as well as coupled cluster singe-double perturbative triple or CCSD(T)—the latter of which is restricted to $[HCN_3S_2]_2$), have questioned the existence of DPB in DTTAs,[40] proposing instead that "long chalcogen−chalcogen bonds" best describe the interaction in this ring system. In view of the paucity of experimental evidence, we set out to obtain structural data for the DTTA dimer **3** that was previously synthesized, because this dimer has already been characterized in solution.[38] Thus, using ^{1}H NMR, it was shown that the only species present in (very dilute) solutions of **3** is a dimer wherein the two 3-CF_3-C_6H_4 rings are π-stacked as in cyclophanes, as indicated by position-dependent shifts to higher frequencies.[38] This specific DTTA is of further interest because of our recently reported work on the structure of 3-CF_3-C_6H_4-CN_2S_2 **6**, that is, the similarly substituted DTDA, which dimerizes in two different motifs (**I** and **II** from Scheme 1) within a single crystal structure.[41] Herein, we now report that **3** indeed adopts the *cis*-coplanar geometry in crystalline lattices and that it has the *anti* disposal of the 3-CF_3 groups that was implied from the symmetry of the NMR spectra. Furthermore, to assess the likelihood that other structural motifs for DTTAs could be operative, we have undertaken a detailed structural investigation using DFT computational methods. Our work confirms previous results indicating the importance of including dispersion-correction terms to accurately predict the binding energies in such dimers.[40] Indeed, we found that without dispersion correction, the common DFT methods are unable to accurately reproduce even the structures of DTTA dimers. Using dispersion-corrected DFT, we have evaluated the relative energies of five different dimer conformations that could plausibly compete with that observed in the crystal structures of **1**−**3**.

DOI: 10.1021/acsomega.8b03211
ACS Omega 2018, 3, 18170−18180

Finally, we reflect on the pros and cons of using DPB to describe DTTA dimers.

RESULTS AND DISCUSSION

Synthesis. Compound **3** is prepared by the literature procedure in a two-step process (Scheme 2) wherein the

Scheme 2. Two-Step Preparation of Compound 3

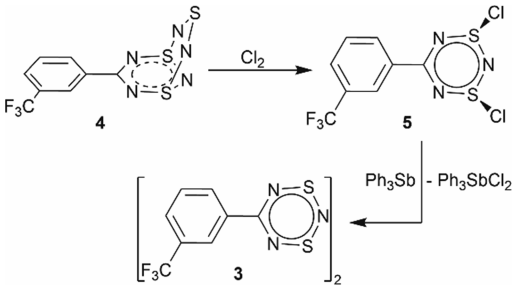

corresponding thiazyl RCN_5S_3 cage compound **4** suspended in CCl_4 is reacted with gaseous Cl_2, which leads in high yield to the thermally unstable S,S-dichloride **5**.[38] Reduction of **5** is best undertaken in rigorously freeze−thaw (3×) degassed $CHCl_3$ using the effective reducing agent Ph_3Sb under conditions where the byproduct Ph_3SbCl_2 remains in solution. Dark-red plates of crystalline **3** form directly from the synthesis reaction if attention is paid to the correct temperature and solvent volumes.

Crystallography. Crystals suitable for X-ray crystal structure determination were obtained for **3** and **4**, whereas the thermal instability of **5** foiled attempts to obtain a crystal structure for this compound. The structural results are depicted in Figures 2 and 3, respectively; full crystallographic

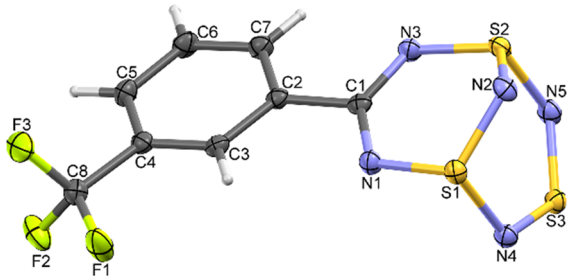

Figure 2. Displacement ellipsoid plot (50%) of **4** in the crystal lattice at 100 K. The atom numbering scheme is shown, and H atoms are drawn with arbitrarily small radii for clarity.

details are provided in Supporting Information. The cage structure of **4** is similar to that of the 16 related structures found in the Cambridge Structure Database (CSD, updates to November 2017).[42] These other structures include a number of different substituents at C1, including aryl groups, halogens, trihalomethyls, and *tert*-butyl. Several examples have cocrystallized solvents, and several examples have aromatic solvents that π-stack with an aryl substituent. The intermolecular distances and angles (Table 1) within the CN_5S_3 cage are indistinguishable from those in the published exemplars.

The most interesting feature of **4** is the lattice structure. Whereas all such RCN_5S_3 cages have strong intermolecular interactions, $(\sum r_{vdW} - 0.20)$ Å or less, in their crystal lattices, the propagation of the contacts in **4** is unique. The contacts do

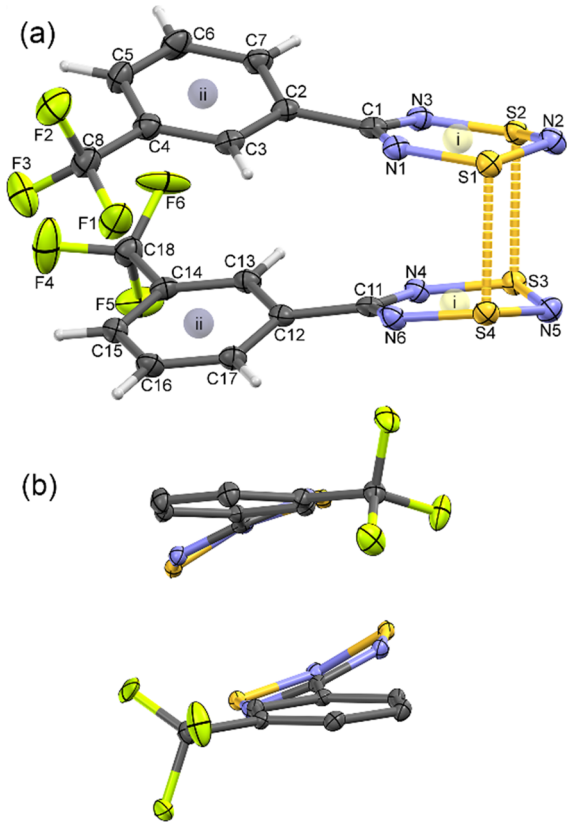

Figure 3. Displacement ellipsoid plots (50%) for the dimer of **3** in the crystal lattice at 100 K. (a) The atom numbering scheme is shown; H atoms are drawn with arbitrarily small radii. Yellow spheres labeled i and gray spheres labeled ii indicate the ring centroid positions for the DTTA and phenyl rings, respectively. Centroid−centroid distances: i···i′ = 2.759; ii···ii′ = 3.850 Å. (b) Side view showing the aryl ring coplanarity. Only the major component of disordered C18 CF_3 group is shown (see Figure S1).

not appear to fall within the purview of chalcogen bonding, and N lone pair-type donors interact with perpendicular p orbitals of the sp^2 hybridized ring C and N═S═N S atoms. Thus, the characteristic $\delta_S^+\cdots\delta_N^-$ interactions are associated with the electron-rich nature of the thiazyls, and their origin therefore probably lies with London forces (see Supporting Information for further information).

The structure of dimer **3** as found in the crystal lattice is depicted in Figure 3 and possesses a similar *cis*-cofacial arrangement of the DTTA rings, as previously reported for dimers **1** and **2**. The approach distance between the two rings minimizes the S···S distances, which, at 2.5069(7) and 2.4956(7) Å, are "short" but still 21.4% longer than a single (σ) bond (2.04 Å) and $-0.85(1) < \sum r_{vdW} = 3.35$ Å (25.4%).[39] The DTTA rings are also no longer planar, because the S1−N2−S2 and S3−N5−S4 moieties tip gently out of the CN_2S_2 planes (mean dihedral angle = 17.6(2)°). Apart from this feature, the structure is strongly reminiscent to that of *cis*-cofacial DTDA dimers, except that the pairs of S atoms are drawn in much closer than the mean of 3.12(2) Å, or $-0.48(2) < \sum r_{vdW}$, found for four *cis*-cofacial dimers in the lattice of **6**.[41] To avoid ambiguities (also when comparing to more distorted geometries in alternative, DFT-computed, structure types), in this work, recourse will be taken to the distance i···i′ between ring centroids for the CN_3S_2 rings (2.759 Å; Figure 3).

DOI: 10.1021/acsomega.8b03211
ACS Omega 2018, 3, 18170−18180

Table 1. Selected Interatomic Distances (Å) and Angles (°) in Crystal Structures of 3 and 4 and DFT of 3a

atoms[a]	4	3 (first ring)	3 (second ring)	3a (first ring)[b]	3a (second ring)[b]
S1−N1 (S3−N4)	1.6192(13)	1.6024(16)	1.6117(16)	1.6130	1.6130
S1−N2 (S3−N5)	1.6292(13)	1.6328(17)	1.6209(17)	1.6486	1.6487
S2−N2 (S4−N5)	1.6296(13)	1.6320(17)	1.6355(17)	1.6332	1.6332
S2−N3 (S4−N6)	1.6190(14)	1.6087(17)	1.6058(16)	1.6111	1.6112
N1−C1 (N4−C11)	1.3436(19)	1.344(3)	1.348(2)	1.3386	1.3379
N3−C1 (N6−C11)	1.337(2)	1.340(3)	1.345(3)	1.3379	1.3386
C1−C2 (C11−C12)	1.492(2)	1.486(3)	1.479(3)	1.4790	1.4790
S1−N4 (S1···S4)	1.7437(14)	2.4956(6)		2.5496	
S2−N5 (S2···S3)	1.7440(15)	2.5069(6)		2.5496	
S1−N1−C1 (S3−N4−C11)	119.64(11)	122.87(14)	121.53(14)	123.08	123.09
N1−S1−N2 (N4−S3−N5)	110.49(7)	112.87(9)	113.69(9)	113.25	113.26
S1−N2−S2 (S3−N5−S4)	112.43(8)	117.39(10)	117.85(10)	116.16	116.15
N2−S2−N3 (N5−S4−N6)	110.47(7)	113.54(9)	112.37(9)	113.67	113.67
S2−N3−C1 (S4−N6−C11)	119.65(11)	121.67(14)	123.00(14)	122.89	122.89
N1−C1−N3 (N4−C11−N6)	130.41(14)	128.68(18)	128.46(17)	127.67	127.66
Tip angle S1N2A	33.23(10)	17.46(15)	17.82(14)	17.96	17.96

[a]Second ring is related to the first by C_2 axis. [b]From B3LYP-D3BJ/6-311+G(2d,p) calculations.

Table 2. Geometry Comparisons Illustrating the Importance of Including Dispersion Correction[a]

parameter	X-ray 3	B3LYP 3a′′′′	B3LYP-D3 3a′	B3LYP-D3BJ 3a	M062X 3a″	APFD 3a′′′	CCSD(T)[b]	MR-AQCC[c]
distance i···i′, Å	2.759	2.889	2.834	2.798	2.750	2.747	2.818	2.796
% deviation from experiment		4.7	2.7	1.4	−0.3	−0.4	2.1	1.3
CN_2S_2 tilt angle, °	13.07(7)	16.9	12.5	12.0	14.5	13.1	11.4	10.4
N_2S tip angle, °	17.6(2)	21.8	18.7	18.0	21.9	19.4	17.5	17.6
distance ii···ii′, Å	3.850[c]	4.353	3.612	3.570[b]	3.526	3.511		
% deviation from experiment		+13.1	−6.2	−7.3	−8.4	−8.8		
mean distance to least-squares planes, Å	3.519(3)	4.239	3.4232	3.395	3.308	3.309		
% deviation from experiment		+20.5	−2.7	−3.5	−5.6	−5.9		
ring skew angle, °	113.4	91.8	108.1	107.4	109.3	109.0		

[a]Here, 3 is the experimental dimer structure; 3a−3a′′′′ are dimer geometries computed by the indicated DFT methods. [b]Computed on $[HCN_3S_2]_2$; see ref 40. [c]Computed on $[HCN_3S_2]_2$; see ref 35.

A second significant feature of the structure is the wedge-shaped orientation of the aromatic rings (Figure 3a), which tilt apart with a dihedral angle of 15.35(1)°. A simple one-parameter ring separation is obtained by defining a distance ii···ii′ of 3.850 Å between the two aryl ring centroids. However, the rings are also significantly skewed (Figure 3b). Thus, to compare the degree of aryl ring separation to the ∼3.50 Å found in strongly π-stacked interactions between strictly nonbonded aryl rings on adjacent aromatic hydrocarbons,[43] a more representative interannular parameter is required. If the C2 → C7 and C12 → C17 phenyl rings are each defined by least-squares planes, then it is possible to determine the range of distances of the opposite ring atoms to each plane from 3.120(3) to 3.922(3) (mean = 3.518 Å). Thus, tethered to the strongly binding DTTA rings, the phenyl rings seem to balance repulsive and attractive dispersion forces and achieve an average separation very close to that predicted for π-stacking and do so by being significantly rotated from the attached CN_2S_3 rings (mean of the torsion angles = 7.7(2)°). This torsion allows the rings to skew (centroids are disposed 23.4° from fully aligned; see Table 2 and Figure 3b). Of course, it is important not to overinterpret such geometries in a crystal structure (for a discussion of the significant crystal packing forces, see Supporting Information), so the solution (from NMR) and gas-phase structures (for the computation, see below) should also be considered.

Now consider what effect the obvious repulsions between the aryl rings have on the tilt angles of the thiazyl rings to which they are attached. We define a least-squares plane through the flat CN_2S_2 portions of each of the rings in the crystal structure of 3. These have an angle of 13.07(7)° between them (so that the phenyl groups each bend further outward about 2° at the attachment point). By comparison, in high-level CCSD(T) computed structures of the "parent" $[HCN_3S_2]_2$ dimers,[35,40] which also show a similar tilted geometry because the S atoms make the closest interannular approach, this angle is 11.4°, whereas MR-AQCC(4,4)/6-311++G(2d,2p) predicts 10.4°.[35] Thus, the net aryl ring repulsion (and steric effects of the CF_3 substituents) on the wedge-shaped structures of DTTA dimers appears to be small but not negligible. For comparison with the dimer of $PhCN_3S_2$ (CSD refcode: DESSID), this angle is 12.5°,[34] whereas with the dimer of 4-$ClC_6H_4CN_3S_2$ (refcode: PAFLAJ), it is 12.6°;[38] both could be expected to have smaller substituent steric effects than 3. The implications of the above factors on the choice of isomer and overall geometry are addressed by DFT computational work (see below).

Solution Structure. The known DTTAs, despite being small, light-atom molecules, have been reported to be very insoluble.[34,38,44] This is likely a consequence of strong association into dimers as well as significant interdimer contacts in the solid lattices (see Supporting Information).

DOI: 10.1021/acsomega.8b03211
ACS Omega 2018, 3, 18170−18180

By contrast, comparably substituted DTDA dimers are highly soluble species in a range of mid- to low-polarity solvents, possibly because of an equilibrium involving dissociation into monomers.[24] It is therefore challenging to determine the structures of DTTAs in solution, but **3** was found to be sufficiently soluble in $CDCl_3$ to allow ^1H NMR spectra to be determined.[38] By comparing with the analogous alkene adducts that are monomeric in solution and in the solid state, it was concluded that these aryl-DTDAs preserve the wedge-shaped structure in solution, similar to that seen in Figure 3. This conclusion is based on the high-frequency shifts of the signals similar to that observed for cyclophanes—the ring H atoms experience a net anisotropic shielding effect from the neighboring ring. Moreover, the observed ^1H signals have symmetry that is consistent with the *anti* disposition of the CF_3 substituents, also as in Figure 3.

Computational Investigation. *Role of Dispersion and Method Verification.* In a recent paper, Mou et al. performed careful and very extensive validations of more than 50 DFT functionals for their ability to reproduce the geometry and binding energy of the *cis*-cofacial $[HCN_3S_2]_2$ isomer of the parent DTTA ring[15] using the MR-AQCC high-level values previously determined by this same research group as reference geometry. Using their criteria, about 15% of the tested methods fit a dimer energy threshold of ±42 kJ mol^{-1}, whereas 59% predicted the S···S separation distance to within 0.1 Å. These criteria limited the number of recommended methods for DTTAs to a small list of 10 standard and 6 dispersion-corrected DFT functionals; the "best method" recommended for both geometry and energy is standard O3LYP.[45] Unfortunately, by using only the hypothetical HCN_3S_2 heterocycle in these tests, the suitability of these methods for experimentally verifiable compounds was not investigated. Thus, when we applied recommended B3LYP in conjunction with double-ζ 6-31+G(2d,p) and triple-ζ 6-311+G(2d,p) basis sets, a very unrealistic geometry resulted, in which the aryl rings are spread too far apart (centroids separation ii···ii′ = 4.353 Å; see Figure 4a). With O3LYP/6-311+G(2d,p), in this work, the geometry converged at an extreme of ii···ii′ = 4.717 Å, causing a 26.7° tilt angle between upper and lower rings, that is, grossly distorting the DTTA dimer. Thus, we turned to dispersion-corrected methods to deal with this unrealistic repulsion of the aryl rings.

We were able to validate a limited number of dispersion-corrected methods, and the results from fully optimized DFT/6-311+G(2d,p) calculations verified to have zero imaginary frequencies are listed in Table 2. In view of the good performance of B3LYP in the energy criterion of Mou et al.,[15] we included both the original B3LYP-D3 and the now-recommended B3LYP-D3BJ methods of Grimme.[46−48] We also tried out M062X,[49] which is widely used for main group inorganic compounds because it has built-in dispersion correction and also the APFD method that is now recommended for use with Gaussian 16.[50]

All the dispersion-corrected methods that were tried significantly reduced the phenyl ring separation (distance ii··· ii′ in Table 2); at the same time, the binding between thiazyl rings is more accurately estimated (distance i···i′). The latter seems to indicate that dispersion effects operate alongside DPB in the thiazyl core dimerization, although a contribution from reduced strain induced by phenyl ring repulsions in the standard DFT-calculated geometries cannot be ruled out. Note, however, that all these methods somewhat overbind the

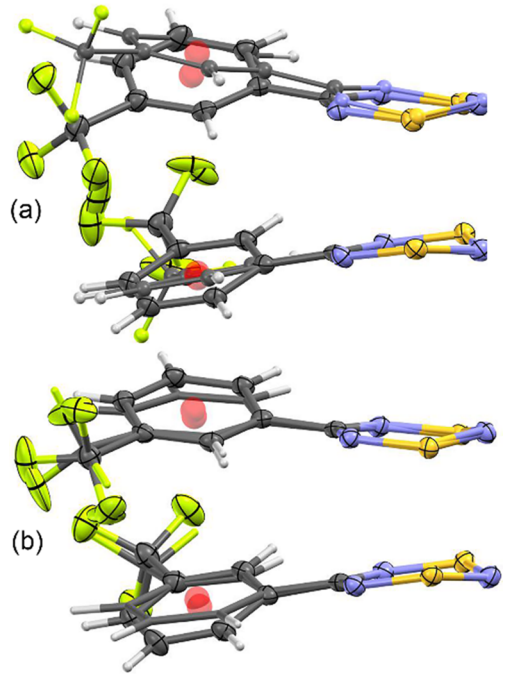

Figure 4. Overlay diagrams of the experimental structure, shown as displacement ellipsoids, of **3** with the results, shown as ball and tube, from (a) standard [B3LYP/6-311+G(2d,p)] **3a**′′′′ and (b) dispersion-corrected [B3LYP-D3BJ/6-311+G(2d,p)] **3a** calculations.

aryl groups so that the distance ii···ii′ is now shorter than in experiment by 6.2−8.8%. Intriguingly, with the use of these methods, the relative conformation adopted by the two 3-$CF_3C_6H_3$ rings is also significantly improved (see Figure 4b). They much more closely match the crystal structure geometry with respect to inter-ring separation, torsion angle to the CN_2S_3 rings, and the skewing of aryl ring centroids (Table 2). We have therefore calculated for each result the average perpendicular ring separation, as discussed above for the crystal structure, and this value and its % deviation from the experimental value are also listed in Table 2. From this limited comparison set, we selected the (U/R)B3LYP-D3BJ empirically corrected dispersion functional in conjunction with the triple-ζ 6-311+G(2d,p) basis set for all further work in this study as the best compromise between accuracy of thiazyl and aryl ring separations and orientation. Moreover, compared to the other methods, it was proven to be computationally more efficient by a significant margin.

Using this adopted method, we then verified the electronic structure of the computed dimer **3a** in this *cis*-cofacial geometry. Frontier molecular orbitals (FMOs) are presented in Figure 5. Both in orbital topologies and relative energies, the electronic structure using this modern DFT method strongly corroborates the bonding picture developed earlier using empirical and semiempirical approaches (Figure 1).[32−34] Thus, the concept of diffuse $\pi^*-\pi^*$ interactions still appears to be very relevant to a description of the electronic structure of strongly binding DTDA dimers such as **3a**. The final electronic structure is thus consistent with a face-to-face association of monomers that either have a triplet ground state or from singlet ground states with easily populated biradicaloids. There is also nothing substantively new from these DFT calculations compared to much earlier STO-3G* calculations.[51] Nevertheless, in view of reports in the literature from high-level

DOI: 10.1021/acsomega.8b03211
ACS Omega 2018, 3, 18170−18180

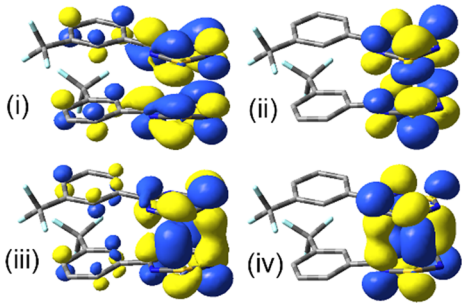

Figure 5. Kohn−Sham orbital hypersurfaces for the FMOs of **3a** from B3LYP-D3BJ/6-311+G(2d,p) DFT calculations: (i) LUMO+1, (ii) LUMO, (iii) HOMO, and (iv) HOMO-1.

wave-function theory (WFT) calculations,[40] we also included the monomers as part of our investigation.

*Computed Monomers **3m**−**3o**.* In their critique of DPB, Haberhauer and Gleiter argue from the relative CCSD(T) computed energies of monomeric DTTA HCN_3S_2.[40] Because **3** is made by the reductive dechlorination of monomeric **5**, it is reasonable to assume that the dimers form through the association of monomeric DTTA moieties, although such species have never been isolated or characterized. By contrast, in isoelectronic EN_3S_2 heterocycles, closely related species in which the RC component of the structure is replaced by either an $E = R_2P$ or $E = \{O_2S\}^-$ moiety, stable antiaromatic monomeric species have been verified both in solution and in the solid state.[52] Crystal structures have been reported for at least five exemplars (Chart 2; CSD refcodes: CANWUJ,[53] DEVCUD,[54] NIPHDS,[55] NSIAPS,[56] and PIZXIF[57]). The most extensively studied of these intriguing compounds is $Ph_2PN_3S_2$ (NIPHDS), but this is the only one to have an almost planar geometry in its crystal structure. This deep purple-colored compound is thermally stable but has a fascinating reactivity; moreover, it can be purified in air using size-exclusion chromatography.[52] The other structures, all bearing more electron-donating substituents at the heteroatom, present with rings that are strongly folded across *trans*-disposed N and S atoms (Chart 2).

Chart 2. Monomeric (Hetero)DTTA Geometries from Crystallography and DFT Calculations

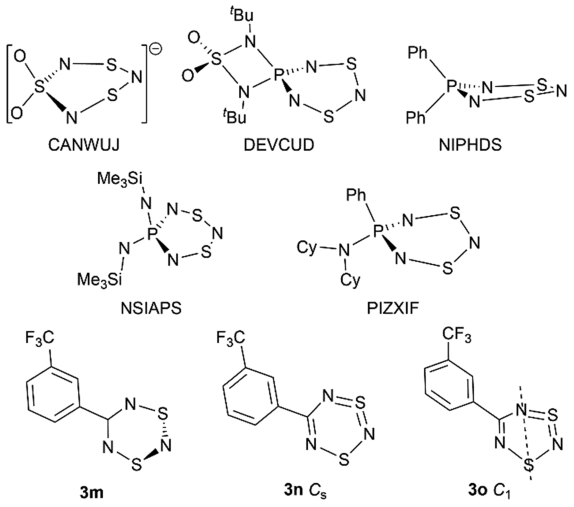

Very briefly, we have calculated fully optimized structures using B3LYP-D3BJ/6-311+G(2d,p) for the triplet monomer **3m** (relative energy of +5.21 kJ mol^{-1}), singlet-C_s monomer **3n** (relative energy of +6.02 kJ mol^{-1}), and singlet-C_1 monomer **3o** (most stable). The C_s (planar) **3n** has an imaginary frequency that distorts toward the C_1 geometry when using triple-ζ basis sets.[51] The resultant structures (Chart 2) include **3m** as almost planar except for a very mild tipping of the terminal SNS moiety (dihedral angle = 10.5°); interestingly, this structural motif can be recognized in both experimental **3** and computed dimers **3a** such that these DTTAs present geometrically as the dimers of triplet-state monomers. Planar **3n** has shorter and longer bond lengths with a distinct N═S═N component, whereas the stable singlet **3o** has a noticeably folded structure (folded about the dashed line shown in Chart 2). This calculated geometry for **3o** is quite similar to that adopted by the four hetero-DTTAs with donor substituents (CANWUJ,[53] DEVCUD,[54] NSIAPS,[56] and PIZXIF[57]). At our level of theory, the calculated energy differences between these three monomer geometries (**3m**−**3o**) amount to less than kT under ambient conditions.

Alternative Dimerization Modes. Published CCSD(T) calculations, also undertaken with HCN_3S_2 moieties, identified additional binding modes for DTTA dimers.[40] There is as yet no experimental evidence for the existence of such structures, but the possibility should be given serious consideration because the radical dimers of DTDAs $[RCN_2S_2]_2$ have the five verified structural motifs shown in Scheme 1. We therefore investigated alternative isomers of computed geometry **3a**, and the results are presented in Table 3 and Figure 6. An obvious alternative geometry is one where the aryl rings are rotated such that the CF_3 groups are *syn* rather than *anti*. Although, intuitively, this might be thought to suffer from increased steric interactions, such *syn* isomers of 3-substituted aryl DTDA dimers with a *cis*-cofacial structure are well attested to in the literature.[26,41] Our computations successfully optimize rotamer **3b** at a mere 7.0 kJ mol^{-1} higher in energy. Significantly, the pairs of aryl rings in both **3a** and **3b** are oriented with a similar degree of coplanarity and have quite similar centroid separations.

The C_{ipso}−i−i′−C_{ipso} torsion angles of computed **3a** and **3b** are 3.7° and 4.8°, respectively. Because many DTTA dimers have such intermediate torsion angles, the utility of generic terms *cis* and *trans* is questionable. Hence, we now introduce alternative designations for the cofacial isomers (Table 3) based on these torsion angles. All these alternative geometries could be minimized using the B3LYP-D3BJ/6-311+G(2d,p) method as fully optimized without imaginary frequencies (Figure 6). They can differ significantly in geometry even when their relative energies are close. For example, *anti*-cofacial-64 **3c** (relative to the CN_3S_2 centroids, +26.7 kJ mol^{-1}) comprised one heavily distorted DTTA ring connected via a short S···N contact of 2.075 Å (17% longer than an S−N single bond of 1.77 Å), connected to a second that has the geometry of the triplet monomer **3m** (Figure 6c).

In stark contrast to this, the cofacial-150 isomers **3d**, **3d′**, and **3d″**, which differ only in the orientations of the CF_3 groups (+26.3 to +27.0 kJ mol^{-1}), have almost planar CN_3S_2 rings and a shortest S···S contact of 2.689 Å (32% longer than an S−S single bond of 2.04 Å). Unlike in **3a** and **3b**, the remote location of the CF_3 groups in this isomer has almost no effect on energetics or geometry. In contrast to the three cofacial isomers **3a**, **3c**, and **3d**, the two antarafacial

DOI: 10.1021/acsomega.8b03211
ACS Omega 2018, 3, 18170−18180

Table 3. Computed Energies and Geometries of Alternative Dimerization Modes for 3[a]

code	geometry	relative E, kJ mol^{-1}	dimerization E, kJ mol^{-1}	distance i···i, Å	distance S···S[b], Å	torsion[c], °
3	experimental			2.759[d]	2.5013(8)	0.5
3a	*anti*-cofacial-4	0.0	−154	2.798[d]	2.5496	3.7
3a′	(DFT only)	7.0	−147	2.892	2.5618, 2.5623	0.1
3b	*syn*-cofacial-5	7.0	−147	2.796[d]	2.5493, 2.5500	4.8
3c	*anti*-cofacial-64	26.7	−127.0	2.665	2.0753	63.6
3d	*syn*-cofacial-150	27.0	−126.6	2.773	2.6893	150.2
3d′	*syn′*-cofacial-150[e]	26.3	−127.4	2.775	2.6971	149.7
3d″	*anti*-cofacial-150	26.4	−127.3	2.774	2.6931	150.4
3e	S,S-antarafacial	102.0	−52	3.226	2.4649, 2.4650	180.0
3f	S,N-antarafacial	103.7	−50	3.472	1.8155, 2.5244	155.3[f]

[a]For structure diagrams, see Figure 6. [b]In **3c** and **3f** (first entry), N···S. [c]Torsions defined as C_{ipso}−i−i′−C_{ipso}. [d]Distance ii···ii: 3.850 Å in **3**; 3.570 Å in **3a**, 3.633 Å in **3b**. [e]*Syn*-150 and *syn′*-150 differ in whether the short S···S contact is adjacent to the two CF_3 groups or opposite to them. [f]A more meaningful torsion for **3f** might be about the N···S axis (167.3°).

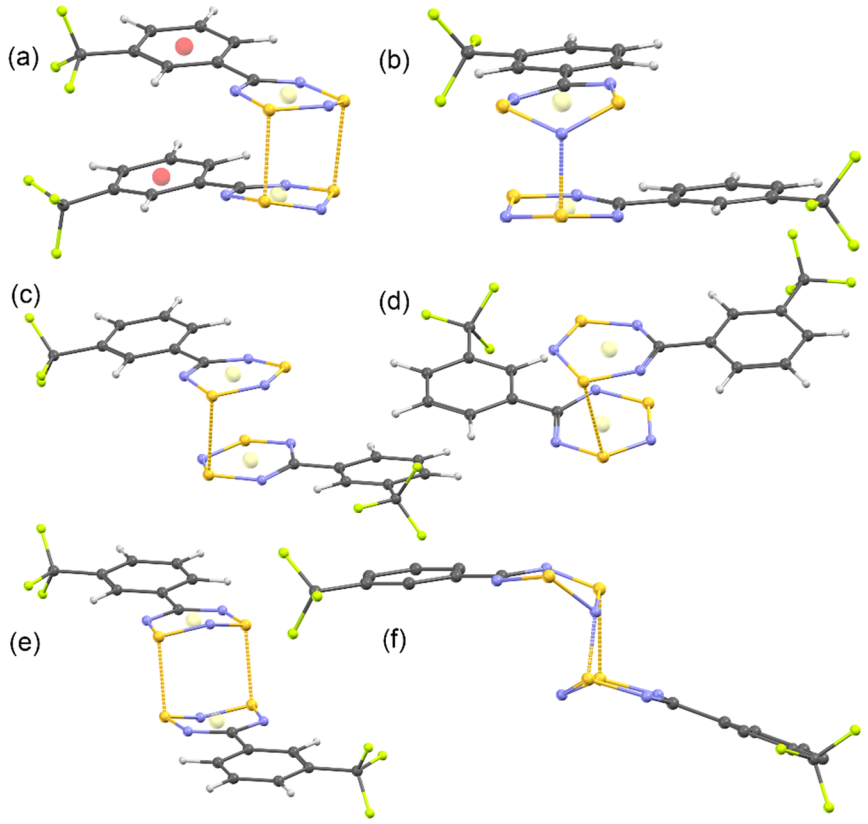

Figure 6. B3LYP-D3BJ/6-311+G(2d,p) calculated geometries of some conceivable structural isomers of **3**: (a) *syn*-CF_3 conformation of cofacial-5 **3b**, (b) *anti*-cofacial-64 **3c**, (c) *syn*-cofacial-150 **3d**, (d) *syn′*-cofacial-150 **3d′**, (e) *trans* S,S-antarafacial isomer **3e**, and (f) *syn* S,N-antarafacial **3f** geometry formed by rotation of **3c** around the short N···S contact.

dispositions are considerably less stable. The rather unlikely looking **3f** geometry is obtained from **3c** by twisting about the S···N contact and retains the more distorted ring shapes of the latter. By contrast, *trans*-antarafacial **3e**, with two tantalizingly short S···S contacts (2.465 Å, 29% longer than covalent single bonds) and a torsion angle of 180.0°, has both CN_3S_2 rings quite similar to that of **3m** but with a higher S_2N tip angle (30.2°compared to 18.0° in **3a**). However, the relative energies of **3e** and **3f** are almost identical (+102.0 and +103.7 kJ mol^{-1}, respectively). Although all five basic shapes are net binding with regard to the monomers, the cofacial isomers that maximize DPB are heavily favored energetically. Finally, it seems highly likely that the main energetic advantage of **3a** over **3c** and **3d** is the stabilizing influence of the aryl-aryl and aryl-CF_3 dispersion forces, in agreement with earlier predictions.[40] In Table S11, we report equivalent data to that in Table 3 for the optimized geometries of dimers of the corresponding prototypical ring HCN_3S_2 **7**. Unlike the CCSD(T) results previously reported, using our standard method, the cofacial-0 geometry is still the most stable, but cofacial-150 and cofacial-64 are only slightly less favorable at +5.5 and +6.1 kJ mol^{-1}, respectively. The two antarafacial geometries, by contrast, remain significantly disfavored at +65.9 kJ mol^{-1}.

Scheme 3 thus shows both the HOMO and HOMO-1 of the dimer pairs and is based on the full Kohn−Sham orbital isosurfaces determined from the DFT calculations. With respect to a choice between short "covalent" interannular

DOI: 10.1021/acsomega.8b03211
ACS Omega 2018, 3, 18170−18180

Scheme 3. Four Best 1,3,2,4,6-Dithiatriazine Dimer Modes Showing the $\pi^*-\pi^*$ Interactions of HOMO (top) and HOMO-1 (bottom): Cofacial-4 VI, Cofacial-64 VII, Cofacial-150 VIII, and *trans*-Antarafacial IX

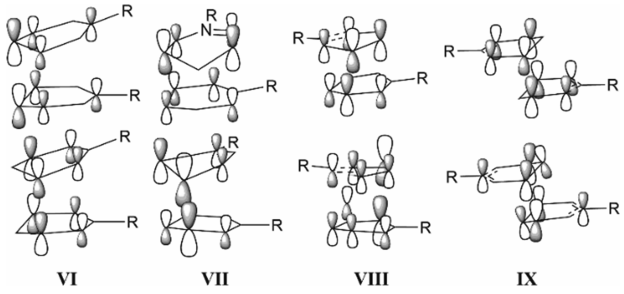

bonds and DPB, there is an overall loss of binding energy of 77 kJ mol^{-1} upon twisting the rings from cofacial to antarafacial. Unlike the situation in DTDAs, the (almost *trans*) cofacial-150 **VIII** is much more favorable than **IX** despite the ability of the latter to form two S···S "bonds". DPB thus seems to be a very reasonable description for the three better binding modes **VI**–**VIII** (Scheme 3), which "lock in" the phase orientation of the π-orbitals in at least one of the two interacting FMOs. Further speculation on these alternative geometries is not warranted at present in the absence of experimental evidence for their existence.

Beyond the three structurally attested type **VI** DTTA dimers **1**–**3** that have been the subject of this study, the literature references two other compound classes. Thus, $CF_3CN_3S_2$ has been prepared and characterized by spectroscopic means.[44] It is described as an unusually insoluble (in view of its size and fluorine content) red solid that decomposes slowly at room temperature. Nothing further has been reported on the DTTA, but many derivatives have been prepared that confirm the chemical identity of the red solids. There are also similar reports of thermally unstable purple solids for $Et_2NCN_3S_2$ and $^iPr_2NCN_5S_2$, but no structures have been obtained.[58] Thus, experimental verification of the possible structures with different geometries, in systems that lack the additional stabilization afforded by aromatic π-stacking as in **3**, has not yet been possible. In preliminary DFT investigations, it would appear that $[CF_3CN_3S_2]_2$ **8** should exist with binding energies in the range of −120 kJ mol^{-1} with very little preference among type **VI**, **VII**, and **VIII** isomers. By contrast, $[Me_2NCN_3S_2]_2$ dimers **9** are calculated to bind by less than 1 kJ mol^{-1} (see Tables S12 and S13 in Supporting Information).

CONCLUSIONS

When essentially flat rings associate as π-dimers in such a way as to maximize diffuse π-orbital overlap, there is strong computational evidence for an orbital-overlap contribution to the bond energy, often of comparable magnitude to contributions from dispersion, electrostatics, or "charge flipping". This concept is summarized in the term pancake bonding and, hence, also "double" pancake bonding in the case of DTTAs.[24,25,35] When applied to hydrocarbons, the distinctive character of pancake bonding can be unambiguously defined, but when extended to thiazyl heterocycles, which have both highly polarizable π-systems and are less resistant to deformation from the ideal planar geometries for sp^2 hybridization, a more nuanced situation emerges. On balance, the evidence from the structural and computational results described above indicates that "double pancake bonding" represents a useful heuristic for binding in the cofacial geometry **VI** that has been experimentally verified in the solid state and in solution for **1**–**3**. Two other modes of dimerization, cofacial-64 **VII** and cofacial-150 **VIII**, appear competitive with **VI** and are equally fittingly described by DPB. By contrast, antarafacial mode **IX**, which does not fit the concept of DPB, is also energetically not competitive. Furthermore, the major source of the energetic preference for **VI** over **VII** and **VIII**, as observed for dimer **3**, is the dispersion interaction between the aryl substituents, which is estimated here at a non-negligible value of 27 kJ mol^{-1} or 17% of the dimerization energy, although in view of the observed overbinding of $\pi-\pi$ stacked aryl substituents, this energy could be exaggerated. Thus, in addition to further experimental work to confirm dimerization modes for nonaryl DTTAs, more effort is needed to validate the best density functionals that are able to provide accurate geometries by neither overbinding nor underbinding pendant substituents.

EXPERIMENTAL SECTION

Syntheses. The RCN_5S_3 cage precursor **4**, 7-[3-(trifluoromethyl)phenyl]-1λ^4,3λ^4,5λ^4-trithia-2,4,6,8,9-pentaazabicyclo[3.3.1]nona-1(9),2,3,5,7-pentaene, CAS [139101-00-1], was prepared as described in the literature.[38] Crystals suitable for single-crystal X-ray diffraction were obtained by recrystallizing from hot CH_3CN. Similarly, the DTTA dimer **3**, 4,9-bis[3-(trifluoromethyl)phenyl]-1λ^4,2λ^4,6λ^4,7λ^4-tetrathia-3,5,8,10,11,12-hexaazatricyclo-[5.3.1.1^{2,6}]dodeca-1(11),2,4,6(12),7,9-hexaene (CAS [139101-11-4]) was also prepared by the published method.[38] X-ray quality crystals deposit from the reaction medium upon cooling. Infrared spectra were obtained on a Bruker Tensor FTIR spectrometer and found in agreement with the published values; similarly, the MP agreed with the published report within experimental error.

X-ray Crystallography. Single crystals of $C_8H_4F_3N_5S_3$ **4** were obtained by cooling a hot CH_3CN solution. A suitable crystal was selected and mounted using a MiTeGen 100 μm loop and Paratone oil on a SuperNova/Pilatus 200K diffractometer with a Cu X-ray microsource focused by X-ray mirrors. The crystal was kept at 100.01(10) K during data collection. Single crystals of $C_8H_4F_3N_3S_2$ **3** were grown from hot $CHCl_3$. Data was collected in the same manner at 99.98(13) K. Data collection was controlled, and data was processed using CrysAlis Pro release 39.46.[59] Using Olex2,[60] the structure was solved with the ShelXT[61] structure solution program and refined with the ShelXL[62] refinement package by least-squares minimization. Crystal data for $C_8H_4F_3N_5S_3$ (M = 323.34 g/mol): monoclinic, space group $C2/c$ (no. 15), a = 22.90772(16) Å, b = 4.66989(3) Å, c = 22.2724(2) Å, β = 106.6781(9)°, V = 2282.39(3) Å^3, Z = 8, T = 100.01(10) K, μ(Cu Kα) = 6.306 mm^{-1}, D_{calc} = 1.882 g/cm^3, 23,650 reflections measured (8.058° ≤ 2Θ ≤ 155.214°), 2390 unique (R_{int} = 0.0276, R_{sigma} = 0.0108), which were used in all calculations. The final R_1 was 0.0280 ($I > 2\sigma(I)$), and wR_2 was 0.0744 (all data). Crystal data for $C_8H_4F_3N_3S_2$ (M = 263.26 g/mol): triclinic, space group $P\bar{1}$ (no. 2), a = 7.62509(11) Å, b = 8.44847(12) Å, c = 15.92585(16) Å, α = 104.2308(10)°, β = 94.4500(10)°, γ = 103.1503(12)°, V = 958.65(2) Å^3, Z = 4, T = 99.98(13) K, μ(Cu Kα) = 5.289 mm^{-1}, D_{calc} = 1.824 g/cm^3, 37,748 reflections measured (11.102° ≤ 2Θ ≤ 154.986°), 4013

DOI: 10.1021/acsomega.8b03211
ACS Omega 2018, 3, 18170−18180

unique (R_{int} = 0.0533, R_{sigma} = 0.0198), which were used in all calculations. The final R_1 was 0.0385 ($I > 2\sigma(I)$), and wR_2 was 0.1076 (all data). See Supporting Information for further information (Tables S1−S10 and Figures S1−S5). The crystallographic data have been deposited at the Cambridge Crystallographic Data Centre as CCDC 1876932-1876933.

Computational Investigations. The general approach was to do a full optimization at the DFT/6-31+G(2d,p) level with frequency checks, followed by DFT/6-311+G(2d,p). The latter repeatedly displayed imaginary frequencies that correspond to deformations toward the "correct" geometries from the high-compliance WFT methods. Reoptimization starting from statically deformed geometries then led to fully converged DFT/6-311+G(2d,p) geometries without imaginary frequencies. A computed structure of **3** was first conducted with the B3LYP functional; although this optimized fully, the geometry indicated excessive repulsion between aryl substituents. Next, a series of functionals with different approaches for inclusion of dispersion effects were tested, primarily using methods already validated for DTTA dimers in the work of Mou et al. (B3LYP-D3, B3LYP-D3BJ, M062X, O3LYP, and also the new APFD method built into GW16[63]). The most tractable method (good compromise between accuracy and efficiency) was B3LYP-D3BJ, which was thenceforth used for all other calculations in conjunction with the abovementioned double-ζ and triple-ζ Pople basis sets. Cartesian coordinates of all the optimized geometries reported in this work are included in Supporting Information (Table S14).

■ ASSOCIATED CONTENT

Supporting Information

The Supporting Information is available free of charge on the ACS Publications website at DOI: 10.1021/acsomega.8b03211.

Full crystallographic data and discussion of lattice contacts for **3** and **4** and DFT computational results with Cartesian geometry records for all optimized geometries reported in this work (PDF)

CCDC 1876932-1876933 containing the crystallographic data for **3** and **4** (CIF)

■ AUTHOR INFORMATION

Corresponding Author

*E-mail: boere@uleth.ca.

ORCID

René T. Boeré: 0000-0003-1855-360X

Notes

The author declares no competing financial interest.

■ ACKNOWLEDGMENTS

This work was underwritten by ongoing Discovery Grants from the Natural Sciences and Engineering Research Council (NSERC). We are grateful to the University of Lethbridge for purchasing the SuperNova diffractometer for our X-ray Diffraction Facility.

■ REFERENCES

(1) Mulliken, R. S.; Person, W. B. *Molecular Complexes: A Lecture and Reprint Volume*; John Wiley & Sons Inc.: New York, 1969, Chapter 16.

(2) Suzuki, S.; Morita, Y.; Fukui, K.; Sato, K.; Shiomi, D.; Takui, T.; Nakasuji, K. Aromaticity on the pancake-bonded dimer of neutral phenalenyl radical as studied by MS and NMR Spectroscopies and NICS Analysis. *J. Am. Chem. Soc.* **2006**, *128*, 2530−2531.

(3) Fukui, K.; Sato, K.; Shiomi, D.; Takui, T.; Itoh, K.; Kubo, T.; Gotoh, K.; Yamamoto, K.; Nakasuji, K.; Naito, A. Electronic structure of a stable phenalenyl radical as studied by ESR/ENDOR, paramagnetic NMR spectroscopy and SQUID measurements. *Mol. Cryst. Liq. Cryst. Sci. Tech., Sect. A: Mol. Cryst. Liq. Cryst.* **1999**, *334*, 49−58.

(4) Soncini, A. Charge and spin currents in open-shell molecules: A unified description of NMR and EPR observables. *J. Chem. Theory Comput.* **2007**, *3*, 2243−2257.

(5) Tian, Y.-H.; Kertesz, M. Charge shift bonding concept in radical π-dimers. *J. Phys. Chem. A* **2011**, *115*, 13942−13949.

(6) Beneberu, H. Z.; Tian, Y.-H.; Kertesz, M. Bonds or not bonds? Pancake bonding in 1,2,3,5-dithiadiazolyl and 1,2,3,5-diselenadiazolyl radical dimers and their derivatives. *Phys. Chem. Chem. Phys.* **2012**, *14*, 10713−10725.

(7) Braida, B.; Hendrickx, K.; Domin, D.; Dinnocenzo, J. P.; Hiberty, P. C. Multicenter bonding in ditetracyanoethylene dianion: A simple aromatic picture in terms of three-electron bonds. *J. Chem. Theory Comput.* **2013**, *9*, 2276−2285.

(8) Cui, Z.-h.; Lischka, H.; Mueller, T.; Plasser, F.; Kertesz, M. Study of the diradicaloid character in a prototypical pancake-bonded dimer: The stacked tetracyanoethylene (TCNE) anion dimer and the neutral K_2TCNE_2 complex. *ChemPhysChem* **2014**, *15*, 165−176.

(9) Cui, Z.-h.; Lischka, H.; Beneberu, H. Z.; Kertesz, M. Rotational barrier in phenalenyl neutral radical dimer: Separating pancake and van der Waals interactions. *J. Am. Chem. Soc.* **2014**, *136*, 5539−5542.

(10) Fatila, E. M.; Mayo, R. A.; Rouzières, M.; Jennings, M. C.; Dechambenoit, P.; Soldatov, D. V.; Mathonière, C.; Clérac, R.; Coulon, C.; Preuss, K. E. Radical−radical recognition: Switchable magnetic properties and re-entrant behavior. *Chem. Mater.* **2015**, *27*, 4023−4032.

(11) Mills, M. B.; Hollingshead, A. G.; Maahs, A. C.; Soldatov, D. V.; Preuss, K. E. Isomerization of a lanthanide complex using a humming top guest template: A solid-to-solid reaction. *CrystEngComm* **2015**, *17*, 7816−7819.

(12) Cui, Z.-h.; Gupta, A.; Lischka, H.; Kertesz, M. Concave or convex π-dimers: The role of the pancake bond in substituted phenalenyl radical dimers. *Phys. Chem. Chem. Phys.* **2015**, *17*, 23963−23969.

(13) Tian, D.; Winter, S. M.; Mailman, A.; Wong, J. W. L.; Yong, W.; Yamaguchi, H.; Jia, Y.; Tse, J. S.; Desgreniers, S.; Secco, R. A.; Julian, S. R.; Jin, C.; Mito, M.; Ohishi, Y.; Oakley, R. T. The metallic state in neutral radical conductors: Dimensionality, pressure and multiple orbital effects. *J. Am. Chem. Soc.* **2015**, *137*, 14136−14148.

(14) Melen, R. L.; Less, R. J.; Pask, C. M.; Rawson, J. M. Structural studies of perfluoroaryldiselenadiazolyl radicals: Insights into dithiadiazolyl chemistry. *Inorg. Chem.* **2016**, *55*, 11747−11759.

(15) Mou, Z.; Tian, Y.-H.; Kertesz, M. Validation of density functionals for pancake-bonded π-dimers; dispersion is not enough. *Phys. Chem. Chem. Phys.* **2017**, *19*, 24761−24768.

(16) Mou, Z.; Kertesz, M. Pancake bond orders of a series of π-stacked triangulene radicals. *Angew. Chem. Int. Ed.* **2017**, *56*, 10188−10191.

(17) Schwamm, R. J.; Lein, M.; Coles, M. P.; Fitchett, C. M. Bismuth(III) complex of the $[S_4]^{\bullet-}$ radical anion: Dimer formation via pancake bonds. *J. Am. Chem. Soc.* **2017**, *139*, 16490−16493.

(18) Juríček, M. The three C's of cethrene. *Chimia* **2018**, *72*, 322−327.

(19) Bates, D.; Robertson, C. M.; Leitch, A. A.; Dube, P. A.; Oakley, R. T. Magnetic bistability in naphtho-1,3,2-dithiazolyl: Solid state interconversion of a thiazyl π-radical and its N−N σ-bonded dimer. *J. Am. Chem. Soc.* **2018**, *140*, 3846−3849.

(20) Shuku, Y.; Mizuno, A.; Ushiroguchi, R.; Hyun, C. S.; Ryu, Y. J.; An, B.-K.; Kwon, J. E.; Park, S. Y.; Tsuchiizu, M.; Awaga, K. An exotic band structure of a supramolecular honeycomb lattice formed by a pancake π-π interaction between triradical trianions of triptycene tribenzoquinone. *Chem. Commun.* **2018**, *54*, 3815−3818.

(21) Beldjoudi, Y.; Nascimento, M. A.; Cho, Y. J.; Yu, H.; Aziz, H.; Tonouchi, D.; Eguchi, K.; Matsushita, M. M.; Awaga, K.; Osorio-Roman, I.; Constantinides, C. P.; Rawson, J. M. Multifunctional dithiadiazolyl radicals: Fluorescence, electroluminescence, and photoconducting behavior in pyren-1′-yldithiadiazolyl. *J. Am. Chem. Soc.* **2018**, *140*, 6260−6270.
(22) Taponen, A. I.; Wong, J. W. L.; Lekin, K.; Assoud, A.; Robertson, C. M.; Lahtinen, M.; Clérac, R.; Tuononen, H. M.; Mailman, M.; Oakley, R. T. Non-innocent base properties of 3- and 4-pyridyl-dithia- and diselenadiazolyl radicals: The effect of *N*-methylation. *Inorg. Chem.* **2018**, *57*, 13901−13911.
(23) Matsui, H.; Yamane, M.; Tonami, T.; Nakano, M.; de Wergifosse, M.; Seidler, T.; Champagne, B. Theoretical study on third-order nonlinear optical property of one-dimensional cyclic thiazyl radical aggregates: Intermolecular distance, open-shell nature, and spin state dependences. *J. Phys. Chem. C* **2018**, *122*, 6779−6785.
(24) Preuss, K. E. Pancake bonds: π-Stacked dimers of organic and light-atom radicals. *Polyhedron* **2014**, *79*, 1−15.
(25) Kertesz, M. Pancake bonding: An unusual pi-stacking interaction. *Chem.-Eur. J.* **2018**, in press, DOI: 10.1002/chem.201802385.
(26) Haynes, D. A. Crystal engineering with dithiadiazolyl radicals. *CrystEngComm* **2011**, *13*, 4793−4805.
(27) Bryan, C. D.; Haddon, R. C.; Hicks, R. G.; Kennepohl, D. K.; MacKinnon, C. D.; Oakley, R. T.; Palstra, T.; Perel, A. S.; Scott, S. R.; Schneemeyer, L.; Waszczak, J. V.; Cordes, A. W. Molecular Conductors from Neutral-Radical Charge-Transfer Salts: Preparation and Characterization of an Iodine-Doped Hexagonal Phase of 1,2,3,5-Dithiadiazolyl ($[HCN_2S_2]\cdot$). *J. Am. Chem. Soc.* **1994**, *116*, 1205−1210.
(28) Campbell, J.; Klapstein, D.; Bernath, P. F.; Davis, W. M.; Oakley, R. T.; Goddard, J. D. Electronic excitation of the 1,2,3,5-dithiadiazolyl radical. A spectroscopic and theoretical analysis. *Inorg. Chem.* **1996**, *35*, 4264−4266.
(29) Cordes, A. W.; Bryan, C. D.; Davis, W. M.; de Laat, R. H.; Glarum, S. H.; Goddard, J. D.; Haddon, R. C.; Hicks, R. G.; Kennepohl, D. K.; Oakley, R. T.; Scott, S. R.; Westwood, N. P. C. Prototypal 1,2,3,5-dithia-and 1,2,3,5-diselenadiazolyl $[HCN_2E_2]^{\cdot}$ (E = S,Se): Molecular and electronic structures of the radicals and their dimers, by theory and experiment. *J. Am. Chem. Soc.* **1993**, *115*, 7232−7239.
(30) Fairhurst, S. A.; Johnson, K. M.; Sutcliffe, L. H.; Preston, K. F.; Banister, A. J.; Hauptman, Z. V.; Passmore, J. Electron spin resonance study of $CH_3CNSSN^{\cdot}$, $C_6H_5CNSSN^{\cdot}$, and $SNSSN^{+}$ free radicals. *J. Chem. Soc., Dalton Trans.* **1986**, *0*, 1465−1472.
(31) Britten, J.; Hearns, N. G. R.; Preuss, K. E.; Richardson, J. F.; Bin-Salamon, S. Mn(II) and Cu(II) complexes of a dithiadiazolyl radical ligand: Monomer/dimer equilibria in solution. *Inorg. Chem.* **2007**, *46*, 3934−3945.
(32) Oakley, R. T. Cyclic and heterocyclic thiazenes. *Prog. Inorg. Chem.* **1988**, *36*, 299−391.
(33) Oakley, R. T. 1993 ALCAN Award Lecture Chemical binding within and between inorganic rings; the design and synthesis of molecular conductors. *Can. J. Chem.* **1993**, *71*, 1775−1784.
(34) Boeré, R. T.; French, C. L.; Oakley, R. T.; Cordes, A. W.; Privett, J. A. J.; Craig, S. L.; Graham, J. B. Preparation and interconversion of dithiatriazine derivatives: Crystal, molecular, and electronic structure of bis(5-phenyl-1,3,2,4,6-dithiatriazine) $(PhCN_3S_2)_2$. *J. Am. Chem. Soc.* **1985**, *107*, 7710−7717.
(35) Cui, Z.-h.; Lischka, H.; Beneberu, H. Z.; Kertesz, M. Double pancake bonds: Pushing the limits of strong π−π stacking interactions. *J. Am. Chem. Soc.* **2014**, *136*, 12958−12965.
(36) Moock, K. H.; Wong, K. M.; Boeré, R. T. 1,5,2,4,6,8-Dithiatetrazocine. Synthesis, computation, crystallography and voltammetry of the parent heterocycle. *Dalton Trans.* **2011**, *40*, 11599−11604.
(37) Tian, Y-H.; Sumpter, B. G.; Du, S.; Huang, J. Pancake π−π bonding goes double: Unexpected 4e/all-sites bonding in boron- and nitrogen-doped phenalenyls. *J. Phys. Chem. Lett.* **2015**, *6*, 2318−2325.
(38) Boeré, R. T.; Fait, J.; Larsen, K.; Yip, J. Preparation of 1,3,2,4,6-Dithiatriazines with substituted aryl groups and the X-ray crystal structure of the (4-chlorophenyl)dithiatriazine dimer. *Inorg. Chem.* **1992**, *31*, 1417−1423.
(39) Boeré, R. T.; Roemmele, T. L. Chalcogen−Nitrogen Radicals. In *Comprehensive Inorganic Chemistry II*; Reedijk, J., Poeppelmeier, K., Eds.; Elsevier: Oxford, 2013; Vol. *1*, pp 375-411.
(40) Haberhauer, G.; Gleiter, R. Double pancake versus long chalcogen−chalcogen bonds in six-membered C,N,S-heterocycles. *Chem.-Eur. J.* **2016**, *22*, 8646−8653.
(41) Boeré, R. T.; Hill, N. D. D. High Z′ structures of 1,2,3,5-dithiadiazolyls and of 1,2,3,5-diselenadiazolyls containing the first structurally characterized monomeric diselenadiazolyls. *CrystEngComm* **2017**, *19*, 3698−3707.
(42) Groom, C. R.; Bruno, I. J.; Lightfoot, M. P.; Ward, S. C. The Cambridge structural database. *Acta Cryst.* **2016**, *72*, 171−179.
(43) Janiak, C. A critical account on π−π stacking in metal complexes with aromatic nitrogen-containing ligands. *J. Chem. Soc., Dalton Trans.* **2000**, *0*, 3885−3896.
(44) Maggiulli, R.; Mews, R.; Stohrer, W.-D.; Noltemeyer, M.; Sheldrick, G. M. Syntheses, structures and bond relationships in mono- and bicyclic 1,3,2,4,6-dithiatriazines. *Chem. Ber.* **1988**, *121*, 1881−1889.
(45) Cohen, A. J.; Handy, N. C. Dynamic correlation. *Mol. Phys.* **2001**, *99*, 607−615.
(46) Goerigkab, L.; Grimme, S. A thorough benchmark of density functional methods for general main group thermochemistry, kinetics, and noncovalent interactions. *Phys. Chem. Chem. Phys.* **2011**, *13*, 6670−6688.
(47) Kruse, H.; Goerigk, L.; Grimme, S. Why the standard B3LYP/6-31G* model chemistry should not be used in DFT calculations of molecular thermochemistry: Understanding and correcting the problem. *J. Org. Chem.* **2012**, *77*, 10824−10834.
(48) Grimme, S.; Hansen, A.; Brandenburg, J. G.; Bannwarth, C. Dispersion-corrected mean-field electronic structure methods. *Chem. Rev.* **2016**, *116*, 5105−5154.
(49) Zhao, Y.; Truhlar, D. G. The M06 suite of density functionals for main group thermochemistry, thermochemical kinetics, noncovalent interactions, excited states, and transition elements: two new functionals and systematic testing of four M06-class functionals and 12 other functionals. *Theor. Chem. Acc.* **2008**, *120*, 215−241.
(50) Austin, A.; Petersson, G. A.; Frisch, M. J.; Dobek, F. J.; Scalmani, G.; Throssell, K. A density functional with spherical atom dispersion terms. *J. Chem. Theory Comput.* **2012**, *8*, 4989−5007.
(51) Hoffmeyer, R. E.; Chan, W.-T.; Goddard, J. D.; Oakley, R. T. The structures and stabilities of singlet and triplet dithiatriazines: A computational study. *Can. J. Chem.* **1988**, *66*, 2279−2284.
(52) Boeré, R. T.; Oakley, R. T.; Shevalier, M. Thermal stability and fluxional behaviour of bicyclic sulphur−nitrogen structures of formula EN_5S_3 (E = CR, PR_2, or SO_2^-). *J. Chem. Soc., Chem. Commun.* **1987**, *0*, 110−112.
(53) Chivers, T.; Cordes, A. W.; Oakley, R. T.; Pennington, W. T. ^{15}N NMR study of the oxidation of the trisulfur trinitride anion by molecular oxygen: A comparison of the molecular and electronic structures of the $S_3N_3^-$, S_3N_3O- and $S_3N_3O_2$- ions. *Inorg. Chem.* **1983**, *22*, 2429−2435.
(54) Gopalakrishnan, J.; Varghese, B.; Doddi, A.; Rao, M. N. S. A new synthetic route to cyclophosphadithiatriazenes: Synthesis and X-ray structural characterization of the first spirocycle containing thiadiazaphosphetidine and phosphadithiatriazene heterocycles. *Appl. Organomet. Chem.* **2006**, *20*, 880−885.
(55) Burford, N.; Chivers, T.; Cordes, A. W.; Laidlaw, W. G.; Noble, M. C.; Oakley, R. T.; Swepston, P. N. Preparation and molecular and electronic structures of cyclo-1λ^5-phospha-3,5-dithia-2,4,6-triazenes and their norbornadiene adducts. *J. Am. Chem. Soc.* **1982**, *104*, 1282−1290.
(56) Weiss, J. *cyclo*-Tri-μ-nitrido-[bis(trimethylsilylamino)-phosphorus]disulphur. *Acta Crystallogr., Sect. B: Struct. Crystallogr. Cryst. Chem.* **1977**, *33*, 2272−2273.

DOI: 10.1021/acsomega.8b03211
ACS Omega 2018, 3, 18170−18180

(57) Mohan, T.; Thomas, C. J.; Rao, M. N. S.; Aravamudan, G.; Meetsma, A.; van de Grampel, J. C. Cyclic sulfur nitrogen compounds and phosphorus reagents: Part XII. Reactions of S_4N_4 with (2-pyridylamino) phosphines. *Heteroat. Chem.* **1994**, *5*, 19−25.
(58) Chivers, T.; Edelmann, F.; Richardson, J. F.; Smith, N. R. M.; Treu, O., Jr.; Trsic, M. Synthesis and Electronic Structure of the $R_2NCS_2N_3$ Ring: X-ray Crystal Structure of the Ricyclic Compound i-$Pr_2NCS_3N_5$ and Preparation of $R_2NCS_2N_3{\cdot}C_7H_8$ (R = Me, Et, *i*-Pr), $Et_2NCS_2N_2^+Cl^-$, and Salts of the $(R_2NCN)(NSCl)(NS)^+$ Cation. *Inorg. Chem.* **1986**, *25*, 2119−2125.
(59) Rigaku Oxford Diffraction. *CrysAlis Pro 39.46.5.5 software*; Rigaku Corporation: The Woodlands, TX, 2017.
(60) Dolomanov, O. V.; Bourhis, L. J.; Gildea, R. J.; Howard, J. A. K.; Puschmann, H. OLEX2. A complete structure solution, refinement and analysis program. *J. Appl. Cryst.* **2009**, *42*, 339−341.
(61) Sheldrick, G. M. SHELXT−Integrated space-group and crystal-structure determination. *Acta Cryst.* **2015**, *71*, 3−8.
(62) Sheldrick, G. M. Crystal structure refinement with SHELXL. *Acta Cryst.* **2015**, *71*, 3−8.
(63) Frisch, M. J.; Trucks, G. W.; Schlegel, H. B.; Scuseria, G. E.; Robb, M. A.; Cheeseman, J. R.; Scalmani, G.; Barone, V.; Petersson, G. A.; Nakatsuji, H.; Li, X.; Caricato, M.; Marenich, A. V.; Bloino, J.; Janesko, B. G.; Gomperts, R.; Mennucci, B.; Hratchian, H. P.; Ortiz, J. V.; Izmaylov, A. F.; Sonnenberg, J. L.; Williams-Young, D.; Ding, F.; Lipparini, F.; Egidi, F.; Goings, J.; Peng, B.; Petrone, A.; Henderson, T.; Ranasinghe, D.; Zakrzewski, V. G.; Gao, J.; Rega, N.; Zheng, G.; Liang, W.; Hada, M.; Ehara, M.; Toyota, K.; Fukuda, R.; Hasegawa, J.; Ishida, M.; Nakajima, T.; Honda, Y.; Kitao, O.; Nakai, H.; Vreven, T.; Throssell, K.; Montgomery, J. A., Jr.; Peralta, J. E.; Ogliaro, F.; Bearpark, M. J.; Heyd, J. J.; Brothers, E. N.; Kudin, K. N.; Staroverov, V. N.; Keith, T. A.; Kobayashi, R.; Normand, J.; Raghavachari, K.; Rendell, A. P.; Burant, J. C.; Iyengar, S. S.; Tomasi, J.; Cossi, M.; Millam, J. M.; Klene, M.; Adamo, C.; Cammi, R.; Ochterski, J. W.; Martin, R. L.; Morokuma, K.; Farkas, O.; Foresman, J. B.; Fox, D. J. *Gaussian 16*, revision B.01; Gaussian, Inc.: Wallingford, CT, 2016.

DOI: 10.1021/acsomega.8b03211
ACS Omega 2018, 3, 18170−18180